

Steric, Inductive, and Ring-Strain Effects in Chelation Thermodynamics and Kinetics. Reactions of Nickel(II) Ion with N-Alkyl-Substituted Diamino Diamides

趙 敏 勳

Min-Shiun Chao

Abstract

The stability constants of the nickel(II) complexes of 4-methyl-4,7-diazadecanediamide (4-Me-L-2,2,2), 4,7-dimethyl-4,7-diazadecanediamide (4,7-Me₂-L-2,2,2), 4-ethyl-4,7-diazadecanediamide (4-Et-L-2,2,2), and 4-methyl-4,8-diazaundecanediamide (4-Me-L-2,3,2) and the two deprotonation constants of each of these complexes have been determined potentiometrically in 0.10 M NaClO₄ at 25°C. Electronic spectra of these complexes and their deprotonated species formed in aqueous solution were measured and discussed. The complexation and dissociation kinetics of these nickel(II) complexes have been studied by using the stopped-flow technique. The possible pathways for the reactions of nickel(II) with these ligands are discussed. It is proposed that these diamino diamides react with the nickel(II) ion by the stepwise formation of coordinate bonds, where the rate-determining step is the formation of the first nickel-nitrogen bond and the subsequent bonding is rapid. Similarly, the dissociation mechanism proposed involves the preequilibration of intermediately bonded species, with the second nickel-nitrogen bond breakage as the rate-determining step. The reactivity order for the dissociation reaction is $\text{Ni}(4\text{-Me-L-2,3,2})^{2+} > \text{Ni}(4,7\text{-Me}_2\text{-L-2,2,2})^{2+} > \text{Ni}(4\text{-Me-L-2,2,2})^{2+} > \text{Ni}(4\text{-Et-L-2,2,2})^{2+}$. The thermodynamic, spectroscopic, and kinetic data are discussed in relation to a combination of steric, inductive, statistical, solvation, and ring-strain effects.

Introduction

Previously, we have reported the thermodynamics and kinetics of the complexation reactions of divalent nickel ion and copper 1-4 ion with four closely related diamino diamides. The ligand, $\text{NH}_2\text{CO}(\text{CH}_2)_n\text{NH}(\text{CH}_2)_m\text{NH}(\text{CH}_2)_p\text{CONH}_2$, is denoted by the symbol L-n, m, p. The current investigation is designed to gain more detailed understanding of the steric, inductive, and ring-strain effects that arise from the substitution at the amino nitrogen donor atom on the thermodynamic, spectra, and kinetic properties of nickel(II) diamino diamide complexes. Thus we have synthesized four new N alkyl-substituted diamino diamides. These ligands are depicted in chart 1. Their complexes with nickel(II) have been studied by potentiometry and visible absorption spectrophotometry, and the reaction kinetics have been studied by stopped-flow methods.

Experimental section

Reagents. The ligands, 4-Me-L-2, 2, 2, 4, 7-Me₂-L-2, 2, 2, 4-Et-L-2, 2, 2, and 4-Me-L-2, 3, 2, where the same as those reported previously. All other chemicals used were of GR grade from Merck or Fluka.

Measurements. For PH measurements a Radiometer PHM 64 instrument equipped with a GK2401B combined electrode was used. The pH was standardized with NBS

buffers. The hydrogen ion and hydroxide ion concentrations in 0.10 M NaClO₄ were calculated from $-\log[\text{H}^+] = \text{pH} - 0.11$ and $K_w = 10^{13.76}$.⁶ Appropriate aliquots of standard solutions of ligand or ligand and metal ion were titrated with a standard CO₂-free sodium hydroxide solution. In all titrations the ionic strength was maintained relatively constant by using 0.10 M NaClO₄ as supporting electrolyte. The solutions were protected from air by a stream of humidified prepurified nitrogen gas and were maintained at $25.0 \pm 0.1^\circ\text{C}$ during the measurements. The methods of calculations are the same as reported previously.¹⁻⁴ The equilibrium constants were obtained by a linear least-squares fit of the data on the CDC Cyber-172 computer.

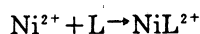
Standard solutions of ligands, borate-mannitol buffers, and sodium perchlorate were prepared by weight. Nickel(II) ion concentration was determined gravimetrically as the DMG complex. The kinetics of the nickel(II) complex formation reactions with 4-Me-L-2, 2, 2, 4, 7-Me₂-L-2, 2, 2, 4-Et-L-2, 2, 2, and 4-Me-L-2, 3, 2, were studied at 368, 374, 382, and 384 nm, respectively, with a Union Giken RA-401 stopped-flow spectrophotometer equipped with a Union RA-415 rapid-scan attachment. For the spectrophotometric experiments the pH was con-

trolled with a borat- mannitol buffer⁶ that was also incorporated into the reference solution. Recrystallized NaClO₄ was used to maintain constant ionic strength at $\mu=0.10$ M in all solutions. Kinetic studies were carried out under pseudo- first- order conditions by using at least a 15- fold excess of ligand concentrations to those of the nickel(II) ion.

Results and Discussion

Composition of the Nickel(II) Complexes. Job's method of continuous variations⁷ was used to determine the composition of the nickel(II) complexes and the results indicated that nickel(II) formed a 1:1 complex with each of these N- alkyl- substituted diamino diamides.

Equilibrium Constants for the Interactions of Nickel(II) with N- Alkyl- Substituted Diamino Diamides. The protonation constants of these ligands have been reported.^{1,4} The reactions of nickel(II) with these ligands are shown in equilibria 1-3, in which L represents the N- alkyl- substituted diamino diamide and the negative subscript on H represents the number of amide protons removed from the complex.



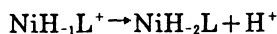
$$K_r = [\text{NiL}^{2+}] / [\text{Ni}^{2+}][\text{L}]$$

(1)



$$K_a = [\text{NiH}_{-1}\text{L}^+][\text{H}^+] / [\text{NiL}^{2+}]$$

(2)



$$K_b = [\text{NiH}_{-2}\text{L}][\text{H}^+] / [\text{NiH}_{-1}\text{L}^+]$$

(3)

The structures of the three complexes NiL²⁺, NiH₋₁L⁺, and NiH₋₂L are shown in Chart II. The equilibrium constants obtained by the methods reported previously^{1, 4} are listed in Table I. For the mixture of Ni²⁺ and 4- Me- L- 2, 3, 2, precipitation forms in basic solution; and the values of K_a and K_b can not be measured accurately. For the purpose of comparison the corresponding values for the equilibrium constants¹ for the reactions of Ni²⁺ with L- 2, 2, 2 L- 2, 3, 2, 5- Me- L- 2, 2, 2, and 6- OH- L- 2, 3, 2 are also given in this table.

The stability constants of these complexes depend heavily on the nature of the diamino diamide, and vary over more than two orders of magnitude in the order Ni(5- Me- L- 2, 2, 2)²⁺ > Ni(L- 2, 2, 2)²⁺ > Ni(4- Et- L- 2, 2, 2)²⁺ > Ni(4- Me- L- 2, 2, 2)²⁺ > Ni(4- Me- L- 2, 3, 2)²⁺ > Ni(6- OH- L- 2, 3, 2)²⁺ > Ni(4, 7- Me₂- L- 2, 2, 2)²⁺ > Ni(4- Me- L- 2, 3, 2)²⁺. This sequence can be explained by a combination of the girdle strins among the three linked chelate rings, the steric

effects of the N-alkyl groups, and the inductive effects of the hydroxyl and the alkyl groups. Like the transition metal complexes of other tetradentate ligands,^{8, 9} the nickel(II) complex of diamino diamides containing 6, 5, 6-membered rings are much more stable than those containing 6, 6, 6-membered rings. The X-ray crystal structures of some nickel(II) and copper(II) complexes of these ligands have been reported¹⁰⁻¹⁸, and the results indicate that the alkyl group attached to the donor nitrogen atom prevents the coordinated diamino diamide from assuming a planar configuration; thus the stability constant of the complex decreases as the number of N-alkyl groups increases.

The stability constants for the copper(II) complexes of these ligands have been reported.^{3,4} For each of these ligands, the stability constants follow the expected Irving-Williams order, Ni(II) < Cu(II). Like the nickel(II) complexes, the stability constant of the copper(II) complex varies in the order [Cu(5-Me-L-2, 2, 2)]²⁺ > [Cu(L-2, 2, 2)]²⁺ > [Cu(4-Et-L-2, 2, 2)]²⁺ > [Cu(4-Me-L-2, 2, 2)]²⁺ > [Cu(L-2, 3, 2)]²⁺ > [Cu(6-OH-L-2, 3, 2)]²⁺ > [Cu(4, 7-Me₂-L-2, 2, 2)]²⁺ > [Cu(4-Me-L-2, 3, 2)]²⁺. This sequence led us to think that there might be a linear relation between the stability constants of

the diamino-diamide complexes of these two metal ions. A plot of log K_f^{Cu} against log K_f^{Ni} gives a straight line as shown in Figure 1. The least-squares equation describing the relation is log K_f^{Ni} = 1.82 log K_f^{Cu} - 1.90. This relationship indicates that stability constants of both copper(II) and nickel(II) complexes are influenced by the same factors, i.e. the steric strains among the three linked rings as well as the steric and the inductive effects of the alkyl and the hydroxyl groups. It is interesting to note that the stability constants of the copper(II) complexes are more sensitive to these factors than the stability constants of the nickel(II) complexes.

The values of K_a and K_b for these nickel(II) complexes obtained by Schwarzenbach's method as previously described¹⁹ are given in Table I along with the corresponding values for the nickel(II) complexes of L-2, 2, 2, 5-Me-L-2, 2, 2, L-2, 3, 2, and 6-OH-L-2, 3, 2. The value of K_a increases in the order [Ni(L-2, 3, 2)]²⁺ < [Ni(6-OH-L-2, 3, 2)]²⁺ < [Ni(5-Me-L-2, 2, 2)]²⁺ < [Ni(L-2, 2, 2)]²⁺ < [Ni(4-Me-L-2, 2, 2)]²⁺ < [Cu(4-Et-L-2, 2, 2)]²⁺ < [Ni(4, 7-Me₂-L-2, 2, 2)]²⁺. Similarly the value of K_b increases in the order [Ni(H₁-L-2, 3, 2)]¹⁺ < [Ni(H₁-6-

OH-L-2, 3, 2)]⁺ < [Ni(H₁-5-Me-L-2, 2, 2)]⁺ < [Ni(H₁-L-2, 2, 2)]⁺ < [Ni(H₁-4-Me-L-2, 2, 2)]⁺ < [Ni(H₁-Et-L-2, 2, 2)]⁺ < [Ni(H₁-4, 7-Me₂-L-2, 2, 2)]⁺. These sequences indicate that the values of both K_A and K_B increase as the girdle strains among the three linked chelate rings decrease and as the number and the size of the N-alkyl groups increase.

The values of K_A and K_B for the copper(II) complexes of these eight diamino diamides have been reported previously.^{3,4,19} For each of these ligands, the value of K_A or K_B increases as the softness of the metal ion increases, i.e. Ni²⁺ < Cu²⁺. The plots of log K_A^{Cu} against log K_A^{Ni} and log K_B^{Cu} against log K_B^{Ni} give straight lines as shown in Figures 2 and 3, respectively. The least-squares equations describing these relations are log K_A^{Cu} = 1.05 log K_A^{Ni} + 0.99 and log K_B^{Cu} = 1.32 log K_B^{Ni} + 3.59, respectively. These relations indicate that K_A and K_B of both copper(II) and nickel(II) complexes are influenced by the same factors, i.e. the girdle strains among the chelate rings as well as the number and the size of the N-alkyl groups.

Electronic Spectra. The absorption spectra of nickel(II)-(4-Me-L-2, 2, 2) solutions are shown in Figure 4. At pH 3.36, the spectrum is the same as that of Ni(ClO₄)₂ (curve 1), practically no complex formation

takes place at this pH. As the pH increases (curves 2 and 3), the intensities of the four bands at 958, 750, 607, and 368 nm increase, reaching a maximum at a=2 (curve 3) due to the formation of Ni(4-Me-L-2, 2, 2)²⁺. Further increase in pH beyond a=2 (curve 4) causes the four absorption bands to shift toward shorter wavelengths due to the Ni-N bond rearrangement and the deprotonation reaction at the amide side (eq 2). At a=2.5 (curve 5), the spectrum has a maximum at about 460 nm. As base concentration is further increased beyond a=2.5 (curves 6-8), this band increases sharply in intensity. Curve 9 is identical with curve 10; these curves are due to the formation of the doubly deprotonated species Ni(H₂-4-Me-L-2, 2, 2). No further changes were observed when the hydroxide ion was added to the solution; this result confirms the potentiometric observation that no further reaction takes place between Ni(H₂-4-Me-L-2, 2, 2) and hydroxide ion.

By the use of the various equilibrium constants listed in Table 1, the degree of formation of Ni(4, 7-Me₂-L-2, 2, 2)²⁺, Ni(H₁-4, 7-Me₂-L-2, 2, 2)⁺, and Ni(H₂-4, 7-Me₂-L-2, 2, 2) in a 1:1 metal-ligand solution as a function of pH can be calculated and is shown in Figure 5. By means of the calculated concentrations of all

species present in each of these solutions, the spectra can be resolved into their components by eq. 4. The absorption characteristics of all species so obtained are given in Table 2.

$$A = b(\epsilon_{\text{NiL}^{2+}}[\text{NiL}^{2+}] + \epsilon_{\text{NiL}^{\text{Ni}^{2+}}}[\text{Ni(H}_1\text{L)}^+] + \epsilon_{\text{NiL}^{\text{NiH}^{-1}}}[\text{Ni(H}_2\text{L)}]) \quad (4)$$

The electronic absorption spectra of NiL^{2+} or $\text{Ni(H}_1\text{L)}^+$ shows four absorption bands, which are assigned to the ${}^3\text{A}_{2g} \rightarrow {}^3\text{T}_{2g}$, ${}^3\text{A}_{2g} \rightarrow {}^1\text{E}_g$, ${}^3\text{A}_{2g} \rightarrow {}^3\text{T}_{1g}$, and ${}^3\text{A}_{2g} \rightarrow {}^3\text{T}_{1g}$ transitions of triplet-ground-state, tetragonally distorted, pseudooctahedral nickel(II) complexes (Table 2);²⁰ while the electronic absorption spectrum of each of these $\text{Ni(H}_2\text{L)}$ species shows a single absorption band in the characteristic 21000–23000 cm^{-1} region, which is assigned to the ${}^1\text{A}_{1g} \rightarrow {}^1\text{E}_g$ transition of singlet-ground-state, square-planar or slightly distorted-planar nickel(II) complex (Table 2).²¹

The potentiometric observation shows two protons of NiL^{2+} are dissociated as the base concentration increases beyond $a=2$ for the 1:1 solution. The spectrophotometric results listed in Table 2 indicate that it is the amide protons, not those of coordinated water molecules, that are dissociated. After the deprotonation reactions and the Ni–O to

Ni–N bond rearrangements at the two amide sites, the in-plane field increases, the extent of axial addition decreases, consequently, $\text{Ni(H}_2\text{L)}$ is a square-planar complex (Table 2).

Comparison of the positions of the ${}^3\text{A}_{2g} \rightarrow {}^3\text{T}_{2g}$ transition for $[\text{NiL}]^{2+}$ or $[\text{NiH}_1\text{L}]^+$ indicates that the ligand field strength decreases in the order $[\text{Ni(L-2, 2)}]^{2+} > [\text{Ni(5-Me-L-2, 2)}]^{2+} > [\text{Ni(6-OH-L-2, 3, 2)}]^{2+} > [\text{Ni(L-2, 3, 2)}]^{2+} > [\text{Ni(4-Me-L-2, 2, 2)}]^{2+} > [\text{Ni(4-Et-L-2, 2, 2)}]^{2+} > [\text{Ni(4, 7-Me}_2\text{-L-2, 2, 2)}]^{2+} > [\text{Ni(4-Me-L-2, 3, 2)}]^{2+}$ and in the order $[\text{Ni(H}_1\text{L-2, 2, 2)}]^+ > [\text{Ni(H}_1\text{5-Me-L-2, 2, 2)}]^+ > [\text{Ni(H}_1\text{6-OH-L-2, 3, 2)}]^+ > [\text{Ni(H}_1\text{L-2, 3, 2)}]^+ > [\text{Ni(H}_1\text{4-Me}_2\text{-L-2, 2, 2)}]^+ > [\text{Ni(H}_1\text{(4-Et-L-2, 2, 2)}]^+ > [\text{Ni(H}_1\text{4, 7-Me}_2\text{-L-2, 2, 2)}]^+$. Comparison of the positions of ${}^1\text{A}_{1g} \rightarrow {}^1\text{E}_g$ transition of $[\text{NiH}_2\text{L}]$ indicates that the ligand field strength decreases in the order $[\text{Ni(H}_2\text{L-2, 2, 2)}] > [\text{Ni(H}_2\text{5-Me-L-2, 2, 2)}] > [\text{Ni(H}_2\text{4-Me-L-2, 2, 2)}] > [\text{Ni(H}_2\text{-Et-L-2, 2, 2)}] > [\text{Ni(H}_2\text{4, 7-Me}_2\text{-L-2, 2, 2)}] > [\text{Ni(H}_2\text{6-OH-L-2, 3, 2)}] > [\text{Ni(H}_2\text{4-Me-L-2, 3, 2)}]$. The two important factors that influence these three sequences are the steric strains among the three linked chelate rings as well as the number and the size

of the N-alkyl groups. As shown in Table III, the ligand field strength decreases as the steric strains among the three linked chelate rings increase and as the number and the size of the N-alkyl groups increase.

Kinetic Results. The kinetics of the complexation reactions of nickel(II) with these N-alkyl-substituted diamino diamides have been studied at 25.0°C, $\mu = 0.10 \text{ M}$ (NaClO_4), and pH 5.58-6.68. Under these conditions these complexation reactions do not proceed to completion. Kinetic studies were carried out under pseudo-first-order conditions by using at least a 15-fold excess of ligand. Plots of K_{obsd} vs. total ligand concentration gave straight lines following eq 5, where $[\Sigma L]$ represents the total concentration of all species of uncomplexed ligand. The slopes are rate constants of

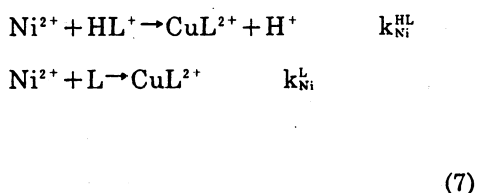
$$k_{\text{obsd}} = k_f[\Sigma L] + k_d \quad (5)$$

complexation, and the intercepts equal the rate constants of dissociation. The values of these rate constants are listed in Table VII. The equilibrium constants calculated from these rate constants by means of eq 6 are in excellent agreement

with those obtained by potentiometric measurements under equilibrium conditions as shown in Table III

$$K = k_f / k_d \quad (6)$$

The kinetic data are found to conform to a reaction scheme in which it is assumed that only the unprotonated and monoprotonated ligand species react at a significant rate (eq 7).



Since proton transfer is very rapid compared to the other reaction steps, this scheme yields the expanded rate expression (eq 8).

$$\begin{aligned} d[\text{NiL}^{2+}] / dt &= k_{\text{Ni}}^{\text{L}}[\text{Ni}^{2+}][\text{L}] + k_{\text{Ni}}^{\text{HL}}[\text{Ni}^{2+}][\text{HL}^+] \\ &- k_{\text{Ni}}^{\text{NL}}[\text{NiL}^{2+}] - k_{\text{H}}^{\text{NL}}[\text{H}^+][\text{NiL}^{2+}] \end{aligned} \quad (8)$$

Combining eq 5 and 8, it is possible to resolve the individual rate constants by plotting the expressions

$$k_f[\Sigma L] / [\text{L}] = k_{\text{Ni}}^{\text{L}} + k_{\text{Ni}}^{\text{HL}}K_1^{\text{H}}[\text{H}^+] \quad (9)$$

$$k_d = k_{\text{Ni}}^{\text{NL}} + k_{\text{H}}^{\text{NL}}[\text{H}^+]$$

(10)

respectively, and the resolved rate constants for each of these systems are listed in Table IV

Kinetics and Mechanism of the Complexation Reactions. Like the complexation reactions of copper(II) ion with these ligands, there are two alternative pathways for the formation of these nickel(II) complexes. As shown in Figure 6, the first step (a→b) for both of these pathways is the diffusion-controlled association of nickel(II) and the ligand. In the next step (b→c), one strongly basic amino nitrogen donor atom of the ligand is presumed to bond to a coordinated water molecule to give a strong outer-sphere hydrogen-bond complex (c). In the first reaction pathway, initial bonding to an amino nitrogen donor atom, the third step (c→d) is the replacement of a water molecule in the inner coordination sphere of nickel(II) by the amino nitrogen atom. This step is the proposed rate-determining step for this pathway, and the subsequent step (d→e) is rapid. In the second reaction pathway (a→b→c→f→g→e), the bonding of the amide oxygen (c→g) occurs first followed by the bonding of an amine nitrogen (f→g) as the rate-determining step; the subsequent step (g→e) is rapid.

The value of k_{Ni}^k decreases in the order L

-2, 2, 2 > L-2, 3, 2 > 4-Et-L-2, 2, 2 > 4-Me-L-2, 2, 2 > 4-Me-L-2, 3, 2 > 4, 7-Me₂-L-2, 2, 2. This sequence is related to two factors: (1) the number of N-alkyl groups and (2) the size of the middle ring. As expected from steric and proximity effects, the rate decreases as the number of the N-alkyl groups increases, and as the size of the middle chelate ring increases. In general, secondary amino nitrogens are more reactive than the tertiary amino nitrogens. The rate-determining steps of the reactions of L-2, 2, 2, 4-Me-L-2, 2, 2 and 4-Et-L-2, 2, 2 are at the complexation of nickel(II) with a secondary nitrogen atom. On the other hand, the rate-determining step for the reaction of 4, 7-Me₂-L-2, 2, 2 is at the complexation of nickel(II) with a tertiary nitrogen atom. Thus, the rate constant for the reaction of 4, 7-Me₂-L-2, 2, 2 is much smaller than those of L-2, 2, 2, 4-Me-L-2, 2, 2 and 4-Et-L-2, 2, 2 as shown in Table IV. The 2-fold decrease of k_{Ni}^k in going from L-2, 2, 2 to either 4-Me-L-2, 2, 2 or 4-Et-L-2, 2, 2 and in going from L-2, 3, 2 to 4-Me-L-2, 3, 2 are due to a statistical effect and an outer-sphere effect.²²

The basicity of the amine group plays a very important role in these reactions. If the activation process is dissociative, the hydrogen bond between the coordinated water and

the amine group of the diamino diamide exists in the transition state; both the K_{Ni} value and the water exchange rate increase as the basicity of the amine group increases.²³ If the activation process is associative, the rate of the formation of the M-N bond increases with the basicity of the amine group.²⁴ In both cases, the rate of complexation increases as the basicity of the amine group increases.

The terminal chelate rings of these complexes are of the same size. If the second reaction pathway (initial bonding to an amide oxygen donor atom $a \rightarrow b \rightarrow c \rightarrow f \rightarrow g \rightarrow e$) were the main reaction pathway, we would expect the formation rate increases as the basicity of the amine group increases, i.e., $k_{Ni}^{L-2,2,2} < k_{Ni}^{L-2,3,2}$ and $k_{Ni}^{4-Et-L-2,2,2} < k_{Ni}^{4-Me-L-2,2,2} < k_{Ni}^{4-Me-L-2,3,2}$. The results listed in Table IV indicate the reverse order and, thus, the main reaction pathway for the reactions of L-2, 2, 2, 4-Me-L-2, 2, 2, and 4-Et-2, 2, 2, is probably the first reaction pathway (initial bonding to an amino nitrogen donor atom $a \rightarrow b \rightarrow c \rightarrow d \rightarrow e$).

As shown in Table IV, protonation causes a large decrease in the formation rate, causing the k_{Ni} ratio to be $(1-7) \times 10^3$. As mentioned above, the ligand basicity is an important rate-controlling factor in an internal conjugate base mechanism. The basi-

city of the monoprotonated diamino diamide is much smaller than that of the unprotonated species. Therefore, the formation rate constant is greatly decreased as a result of protonation because of the ligand basicity, electrostatic repulsion, and statistical effect.²²

Kinetics and Mechanism of the Dissociation Reaction. As shown in Table IV, the dissociation rate constants of these reactions depend heavily on the nature of the diamino diamide, the leaving group. In contrast, the rates of complexation reactions of these complexes display relatively little sensitivity to the nature of the tetradentate ligand, the entering group. These results indicate that, the rate-determining step of the dissociation reaction occurs at the latter stage of the reaction (step III \rightarrow IV and III \rightarrow V in Figure 7).

Without the assistance of acid ($pH > 6$), the main pathway is the water dissociation pathway represented by the sequence I \rightarrow II \rightarrow III \rightarrow IV (Figure 7), where the rate-determining step is the breakage of the second nickel-nitrogen bond (step III \rightarrow IV), and the overall rate constant for this solvent dissociation pathway, k_{NiL} , corresponds to $k_1 k_2 k / k_{-1} k_{-2}$. Individual steps in the unwrapping of the diamino diamide from nickel(II) are not very slow, but unless the

reaction is assisted by acid, the successive equilibria leading up to the cleavage of the second nickel-nitrogen bond are very unfavorable and an extremely slow dissociation rate results.

Below pH6, where acid helps to speed the dissociation reaction by protonation of the released amine group(III→V), the main pathway is the proton-assisted pathway(I→II→III→V→VI). Under the conditions used in this work, $k_4[H^+] < k_{-2}$, thus the rate-determining step for this proton-assisted pathway is the protonation of the released amino group(III→V), and the overall rate constant, k_{IH} , corresponds to $k_1k_2k_4 / k_{-1}k_{-2}$.

The values of both k_{NIL} increase in the order $[Ni(L-2, 2, 2)]^{2+} < [Ni(4-Et-L-2, 2, 2)]^{2+} < [Ni(4-Me-L-2, 2, 2)]^{2+} < [Ni(L-2, 3, 2)]^{2+} < [Ni(4, 7-Me_2-L-2, 2, 2)]^{2+} < [Ni(4-Me-L-2, 3, 2)]^{2+}$. It is significant to note that the order of stabilities of these complexes does not parallel the order of their aqueous solution instabilities. There are two important factors influencing the stability of these complexes: one is the steric strains among the three linked chelate rings and the other, the number of the N-alkyl groups. As shown in Table VIII, the complexes with a 6, 6, 6-membered ring system dissociate much faster than the complexes with a 6, 5, 6-

member ring system. For the complexes with the same chelate ring system the rate of dissociation increases as the number of N-alkyl groups increases. In other words, the breadage of the nickel(II)-tertiary amine bond is faster than that of the nickel(II)-secondary amine bond.

Like the analogous copper(II) complexes, the ratio k_H^{NIL} / k^{NIL} for the nickel(II) complex with a 6, 6, 6-membered ring system is larger than that for the complex with a 6, 5, 6-membered ring system (Table VIII). As shown in Figure 7, the value of k_4 depends significantly on the number of carbon atoms between the two amine groups. As expected from the ligand basicity and the electrostatic repulsion between Ni^{2+} and H^+ , k_4 increases with the number of carbon atoms between the two amine groups. Consequently, the ratio k_H^{NIL} / k^{NIL} for the complex with a 6, 6, 6-membered ring system is significantly larger than that with a 6, 5, 6-membered ring system as shown in Table VIII.

Reference

1. Liu, S.-H.; Chung, C.-S. *Inorg. Chem.* 1984, 23, 1803-1806.
2. Liu, S.-H.; Chung, C.-S. *Inorg. Chem.* 1985, 24, 368-2373.
3. Liu, S.-S. *Inorg. Chem.* 1986, 25, 3890-3806.
4. Chao, M.-S.; Chung, C.-S. *Inorg. Chem.* 1989, 28, 686-692.

5. Bates, R.G. Determination of pH; Wiley: New York, 1964, p74.
6. Margerum, D.W.; Rorabacher, D.B.; Clarke, J.F.G. Inorg. Chem. 1963, 2, 667-677.
7. Drago, R.S. physical Methods in chemistry; Saunders: Philadelphia, 1977, p95.
8. Paoletti, P.; Fabbrizzi, ; Barbwcei, R. Inorg. Chem. 1973, 12, 1861-1864.
9. Wang, B.; Chung, C.-S. J. Chem. Soc., Dalton Trans. 1982, 2565-2566.
10. Lee, T.-J.; Liu, S.-H.; Chung, C.-S. Acta Cryst., C40, 1131-1135.
11. Lee, T.-J.; Liu, S.-H.; Chung, C.-S. Acta Cryst., C40, 1673-1675.
12. Lee, T.-J.; Liu, S.-H.; Chung, C.-S. Acta Cryst., C41, 844-846.
13. Hong, C.-Y.; Chao, M.-S.; Chung, C.-S. Acta Cryst. C43, 34-37.
14. Lu, T.-H.; Chao, M.-S.; Chung, C.-S, Acta Cryst. C43, 207-209.
15. Lu, T.-H.; Chao, M.-S.; Chung, C.-S, Acta Cryst. C43, 661-663.
16. Wang, S.-L; Chang, C.-H.; Chung, C.-S. Acta Cryst. C44, 1719-1722.
17. Lu, T.-H.; Len, C.-H.; Chung, C.-S. Acta Cryst. C45, 13-16.
18. Wu, F.-J. Len, C.-H; Chung, C.-S. Acta Cryst .C45, 1076-1077.
19. Chao, M.-S.; Chung, C.-S. J. Chem. Soc., Dalton Trans. 1981, 683-686.
20. Lee, C.-S; Wu, S.-Y.; Chung, C.-S. Inorg. Chem. 1984, 23, 1298-1303.
21. Chen, J.-w.; Chung, C.-S. Inorg. Chem. 1986, 25, 2841-2846.
22. Chung, C.-S. Inorg. Chem. 1979, 18, 1318-1321.
23. Margerum, D.W.; Cayley, G.R.; Weatherburn, D.C.; Pagenkopf, G.K. In Coordination Chemistry; Martell, A.E., Ed, ; ACS Monograph 174; A American Chemical Society: Washington, D.C. 1978; Vol. 2, pp 1-220.
24. Basolo, F.; Pearson, R.G. " Mechanisms of Inorganic Reactions ", 2nd ed.; Wiley: New York, 1968, p138-141.

Table I. Equilibrium Constants for the Interactions of Diamino Diamides with Nickel(II) at $25.0 \pm 0.1^\circ\text{C}$ and $\mu = 0.10\text{ M}$ (NaClO_4)

ligand	$\log K_f^a$	$\log K_A^b$	$\log K_B^c$
L- 2,2,2 ^d	7.90 ± 0.06	- 8.56	- 9.75
4- Me- L- 2,2,2	7.00 ± 0.06	- 8.71	- 9.71
4- Et- L- 2,2,2	7.13 ± 0.08	- 8.10	- 9.67
4,7- Me ₂ - L- 2,2,2	6.21 ± 0.07	- 7.91	- 9.47
5- Me- L- 2,2,2 ^d	7.95 ± 0.06	- 8.77	- 9.94
L- 2,3,2 ^d	6.82 ± 0.08	- 9.10	- 10.27
4- Me- L- 2,3,2	5.48 ± 0.06	-	-
6- OH- L- 2,3,2 ^d	6.43 ± 0.07	- 8.96	- 10.16

$$^a K_f = [\text{NiL}^{2+}] / [\text{Ni}^{2+}][\text{L}].$$

$$^b K_A = [\text{NiH}_{-1}\text{L}^+][\text{H}^+] / [\text{NiL}^{2+}].$$

$$^c K_B = [\text{NiH}_{-2}\text{L}][\text{H}^+] / [\text{NiH}_{-1}\text{L}^+].$$

^dFrom ref 1.

Table II. Electronic Absorption Spectra of Nickel(II) Complexes of Diamino Diamides in Aqueous Solution

Compound	transition	λ_{\max} , nm	ϵ_{\max} , M ⁻¹ cm ⁻¹
[Ni(4- Me- L- 2,2,2)] ²⁺	³ A _{2g} → ³ T _{2g}	958	27.4
	³ A _{2g} → ¹ E _g	750	4.1
	³ A _{2g} → ³ T _{1g}	607	10.8
	³ A _{2g} → ³ T _{1g}	368	22.7
[Ni(H ₁ -4- Me- L- 2,2,2)] ⁺	³ A _{2g} → ³ T _{2g}	950	23.5
	³ A _{2g} → ¹ E _g	745	3.5
	³ A _{2g} → ³ T _{1g}	603	9.7
	³ A _{2g} → ³ T _{1g}	365	35.4
[Ni(H ₂ -4- Me- L- 2,2,2)]	³ A _{1g} → ¹ E _g	448	108
[Ni(4- Et- L- 2,2,2)] ²⁺	³ A _{2g} → ³ T _{2g}	961	27.8
	³ A _{2g} → ¹ E _g	744	5.8
	³ A _{2g} → ³ T _{1g}	609	11.2
	³ A _{2g} → ³ T _{1g}	382	23.4
[Ni(H ₁ -4- Et- L- 2,2,2)] ⁺	³ A _{2g} → ³ T _{2g}	954	24.1
	³ A _{2g} → ¹ E _g	750	4.9
	³ A _{2g} → ³ T _{1g}	607	9.8
	³ A _{2g} → ³ T _{1g}	368	36.1
[Ni(H ₂ -4- Et- L- 2,2,2)]	¹ A _{1g} → ¹ E _g	449	109

Continued

[Ni(4,7- Me ₂ - L- 2,2,2)] ²⁺	³ A _{2g} → ³ T _{2g}	965	18.7
	³ A _{2g} → ¹ E _g	754	5.6
	³ A _{2g} → ³ T _{1g}	620	11.8
	³ A _{2g} → ³ T _{1g}	374	19.1
[Ni(H- ₄ ,7- Me ₂ - L- 2,2,2)] ⁺	³ A _{2g} → ³ T _{2g}	962	16.1
	³ A _{2g} → ¹ E _g	748	4.8
	³ A _{2g} → ³ T _{1g}	615	10.1
	³ A _{2g} → ³ T _{1g}	370	30.2
[Ni(H- ₂ ,4,7- Me ₂ - L- 2,2,2)]	¹ A _{1g} → ¹ E _{1g}	452	112
[Ni(L- 2,3,2)] ^{2+a}	³ A _{2g} → ³ T _{2g}	915	14.8
	³ A _{2g} → ¹ E _g	750	5.2
	³ A _{2g} → ³ T _{1g}	608	6.4
	³ A _{2g} → ³ T _{1g}	372	12.6
[Ni(H- ₁ - L- 2,3,2)] ^{+a}	³ A _{2g} → ³ T _{2g}	910	12.7
	³ A _{2g} → ¹ E _g	748	4.4
	³ A _{2g} → ³ T _{1g}	604	5.5
	³ A _{2g} → ³ T _{1g}	367	21.7
[Ni(H- ₂ - L- 2,3,2)] ^a	¹ A _{1g} → ¹ E _g	467	100
[Ni(4- Me- L- 2,3,2)] ²⁺	³ A _{2g} → ² T _{2g}	969	21.5
	³ A _{2g} → ¹ E _g	753	5.8
	³ A _{2g} → ³ T _{1g}	635	9.8
	³ A _{2g} → ³ T _{1g}	384	18.6
[Ni(5- Me- L- 2,2,2)] ^{2+a}	³ A _{2g} → ² T _{2g}	905	22.2
	³ A _{2g} → ¹ E _g	745	6.3
	³ A _{2g} → ³ T _{1g}	602	7.8
	³ A _{2g} → ³ T _{1g}	364	15.2

Continued

[Ni(H ₁₅ - Me- L- 2,2,2)] ^a	³ A _{2g} → ² T _{2g}	900	19.1
	³ A _{2g} → ¹ E _g	742	5.4
	³ A _{2g} → ³ T _{1g}	600	6.7
	³ A _{2g} → ³ T _{1g}	361	24.6
[Ni(H ₂₅ - Me- L- 2,2,2)] ^a	¹ A _{1g} → ¹ E _g	442	107
[Ni(6- OH- L- 2,3,2)] ^{2+a}	³ A _{2g} → ³ T _{2g}	908	15.2
	³ A _{2g} → ¹ E _g	746	5.4
	³ A _{2g} → ³ T _{1g}	604	6.8
	³ A _{2g} → ³ T _{1g}	369	13.4
[Ni(H ₁₆ - OH- L- 2,3,2)] ^a	³ A _{2g} → ³ T _{2g}	902	13.1
	³ A _{2g} → ¹ E _g	743	4.7
	³ A _{2g} → ³ T _{1g}	601	5.9
	³ A _{2g} → ³ T _{1g}	365	22.3
[Ni(H ₂₆ - OH- L- 2,3,2)] ^a	¹ A _{1g} → ¹ E _{1g}	462	103
[Ni(L- 2,2,2)] ²⁺	³ A _{2g} → ³ T _{2g}	900	21.6
	³ A _{2g} → ¹ E _g	741	6.2
	³ A _{2g} → ³ T _{1g}	600	8.0
	³ A _{2g} → ³ T _{1g}	363	14.6
[Ni(H ₁₇ - L- 2,2,2)] ^a	³ A _{2g} → ³ T _{2g}	896	18.5
	³ A _{2g} → ¹ E _g	738	5.3
	³ A _{2g} → ³ T _{1g}	597	7.2
	³ A _{2g} → ³ T _{1g}	359	23.2
[Ni(H ₁₇ - L- 2,2,2)] ^a	¹ A _{1g} → ¹ E _{1g}	440	102

^aFrom ref 1.

Table III Rate Constants for Formation (k_f) and Dissociation (k_d) of Nickel(II) Complexes of Diamino Diamides and Equilibrium Constants for the Complexation Reactions of the Nickel(II) Ion with Diamino Diamides at $25.0 \pm 0.1^\circ\text{C}$ and $\mu = 0.10\text{ M}$ (NaClO_4)

Ligand	pH	$k_f, \text{M}^{-1}\text{s}^{-1}$	k_d, s^{-1}	equil const, M^{-1}	
				kinetic ^a	potentiometric
4-Me-L-2,2,2	5.68	63.2	10.55×10^3	5.99×10^3	5.82×10^3
	5.79	31.5	10.15×10^3	8.03×10^3	7.91×10^3
	5.88	97.8	9.76×10^3	1.00×10^4	1.01×10^4
	5.98	128	9.58×10^3	1.34×10^4	1.31×10^4
	6.07	150	9.40×10^3	1.60×10^4	1.65×10^4
	6.19	208	9.18×10^3	2.27×10^4	2.24×10^4
	6.27	250	9.08×10^3	2.75×10^4	2.73×10^4
	6.42	342	8.82×10^3	3.88×10^4	3.94×10^4
	6.54	463	8.73×10^3	5.30×10^4	5.25×10^4
	6.67	615	8.66×10^3	7.10×10^4	7.13×10^4
4,7-Me ₂ -L-2,2,2	5.66	42.3	1.28×10^2	3.30×10^3	3.18×10^3
	5.76	51.6	1.23×10^2	4.20×10^3	4.09×10^3
	5.89	64.5	1.18×10^2	5.76×10^3	5.64×10^3
	5.98	78.3	1.14×10^2	6.87×10^3	7.04×10^3
	6.06	96.2	1.12×10^2	8.59×10^3	8.45×10^3
	6.18	125	1.10×10^2	1.14×10^4	1.13×10^4
	6.27	148	1.08×10^2	1.37×10^4	1.40×10^4

Continued

	6.43	212	1.06×10^3	2.00×10^4	2.02×10^4
	6.54	275	1.04×10^2	2.64×10^4	2.60×10^4
	6.68	378	1.03×10^2	3.67×10^4	3.60×10^4
4- Et- L- 2,2,2	5.58	32.5	8.62×10^3	3.77×10^3	3.71×10^3
	5.68	43.5	8.36×10^3	5.20×10^3	5.4×10^3
	5.76	54.2	7.90×10^3	6.86×10^3	6.78×10^3
	5.85	67.8	7.70×10^3	8.81×10^4	9.02×10^3
	5.96	95.1	7.28×10^3	1.31×10^4	1.26×10^4
	6.07	113	7.18×10^3	1.57×10^4	1.75×10^4
	6.18	179	7.02×10^3	2.55×10^4	2.38×10^4
	6.27	216	6.81×10^3	3.17×10^4	2.06×10^4
	6.41	292	6.71×10^3	4.35×10^4	4.44×10^4
	6.57	415	6.58×10^3	6.31×10^4	6.65×10^4
4- Me- L- 2,3,2	5.81	3.64	2.91×10^1	1.25×10^1	1.40×10^1
	5.90	5.85	2.65×10^1	2.21×10^1	2.07×10^1
	5.99	7.02	2.25×10^1	3.12×10^1	3.05×10^1
	6.09	9.72	2.10×10^1	4.63×10^1	4.67×10^1
	6.18	12.9	1.92×10^1	6.71×10^1	6.83×10^1
	6.30	18.5	1.81×10^1	1.02×10^2	1.11×10^2
	6.42	27.5	1.76×10^1	1.56×10^2	1.80×10^2
	6.54	51.2	1.64×10^1	3.12×10^2	2.83×10^2
	6.67	73.6	1.53×10^1	4.84×10^2	4.60×10^2
	6.79	101	1.48×10^1	6.83×10^2	7.02×10^2

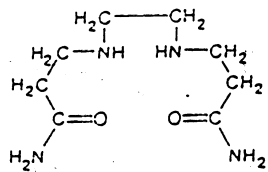
^aKinetically determined value = k_f / k_d .

Table IV Values of Resolved Rate Constants for the Formation and Dissociation of Nickel(II) Complexes of Diamino Diamides in Aqueous Solution at $25.0 \pm 0.1^\circ\text{C}$ and $\mu = 0.10\text{ M}$ (NaClO_4)

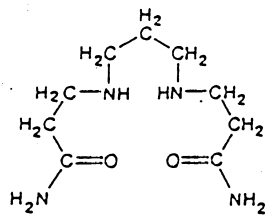
ligand	k_{Ni}^{L} , $\text{M}^{-1}\text{sec}^{-1}$	$k_{\text{Ni}}^{\text{HL}}$, $\text{M}^{-1}\text{sec}^{-1}$	k^{NiL} , sec^{-1}	$k_{\text{H}}^{\text{NiL}}$, $\text{M}^{-1}\text{sec}^{-1}$	$k_{\text{H}}^{\text{NiL}}/k^{\text{NiL}}$ M^{-1}
L- 2,2,2 ^a	1.58×10^5	25.1	2.09×10^{-3}	1.73×10^2	8.28×10^4
4- Me- L- 2,2,2	8.47×10^4	16.2	8.47×10^{-3}	7.96×10^2	9.40×10^4
4- Et- L- 2,2,2	8.62×10^4	17.6	6.39×10^{-3}	6.85×10^2	1.07×10^5
4,7- Me ₂ - L- 2,2,2	1.65×10^4	8.52	1.02×10^{-2}	8.52×10^2	8.35×10^4
L- 2,3,2 ^a	9.55×10^4	33.1	1.41×10^{-2}	8.51×10^3	6.04×10^5
4- Me- L- 2,3,2	4.12×10^4	21.4	1.36×10^{-1}	7.43×10^4	5.46×10^5

^aFrom ref 3.

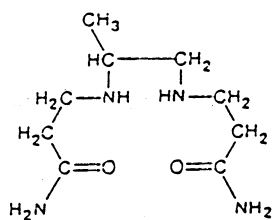
Chart I.



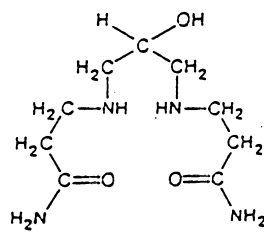
L-2,2,2



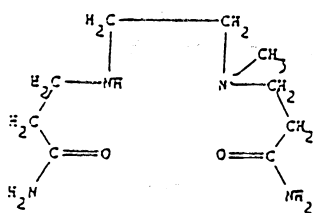
L-2,3,2



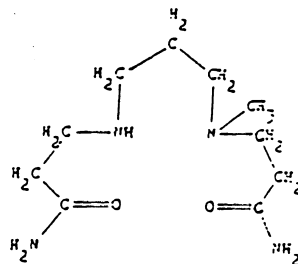
5-Me-L-2,2,2



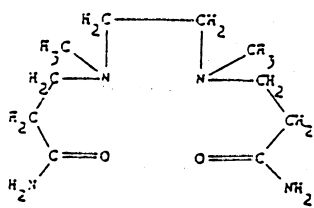
6-OH-L-2,3,2



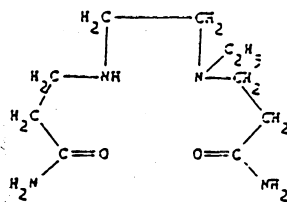
4-Me-L-2,2,2



4-Me-L-2,3,2



4,7-Me₂-L-2,2,2



4-Et-L-2,2,2

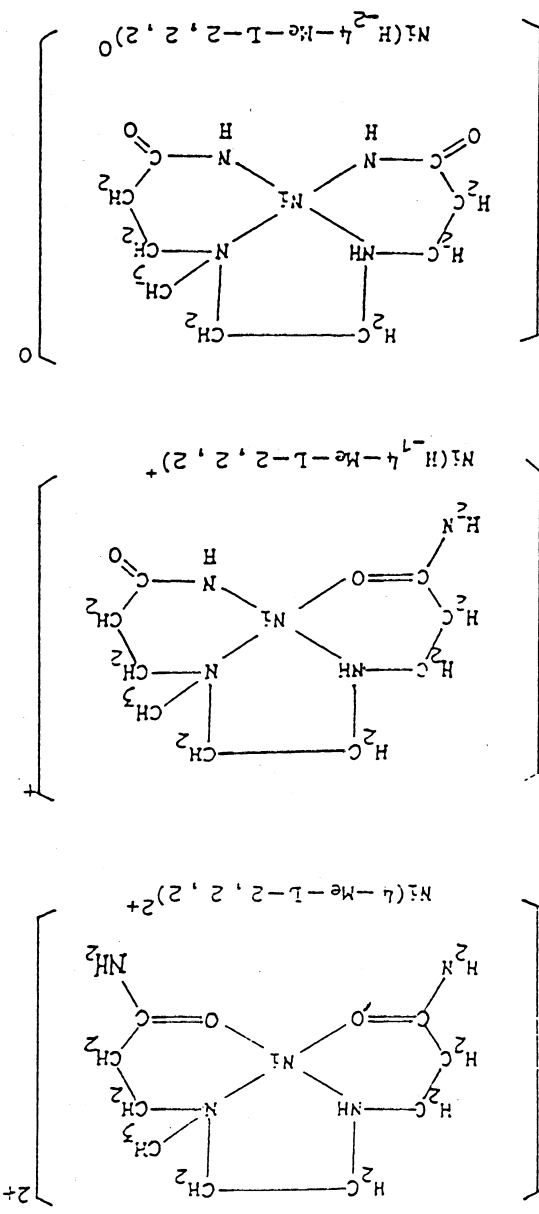


Chart II.

Figure Captions

- Figure 1. Plot of $\log K_f(\text{CuL})$ against $\log K_f(\text{NiL})$ at 25.0°C and $\mu = 0.10\text{ M}$ (NaClO_4).
- Figure 2. Plot of $-\log K_A(\text{CuL})$ against $-\log K_A(\text{NiL})$ at 25.0°C and $\mu = 0.10\text{ M}$ (NaClO_4).
- Figure 3. Plot of $-\log K_B(\text{CuL})$ against $-\log K_B(\text{NiL})$ at 25.0°C and $\mu = 0.10\text{ M}$ (NaClO_4).
- Figure 4. Visible absorption spectra of nickel(II)- (4-Me-L-2,2,2) solutions. All solutions contain $0.00283\text{ M Ni}[\text{ClO}_4]_2$ and $0.00283\text{ M [H}_2\text{4-Me-L-2,2,2][ClO}_4]_2$ at $25.0 \pm 0.1^\circ\text{C}$ and 0.10 M NaClO_4 . The pH values of the solutions are as follows: (1) 3.36; (2) 4.90; (3) 6.91; (4) 8.38; (5) 9.30; (6) 9.97; (7) 10.69; (8) 11.81; (9) 12.02; (10) 12.21.
- Figure 5. Degree of formation of nickel(II)- (4,7-Me₂-L-2,2,2) complexes in 1:1 metal- to- ligand solutions.
- Figure 6. Possible pathways for the reaction of nickel(II) with the unprotonated diamino diamide. The circle represents the division between inner- sphere coordination and outer- sphere association.
- Figure 7. Proposed mechanism for the dissociation reactions of nickel(II)- diamino diamide complexes.

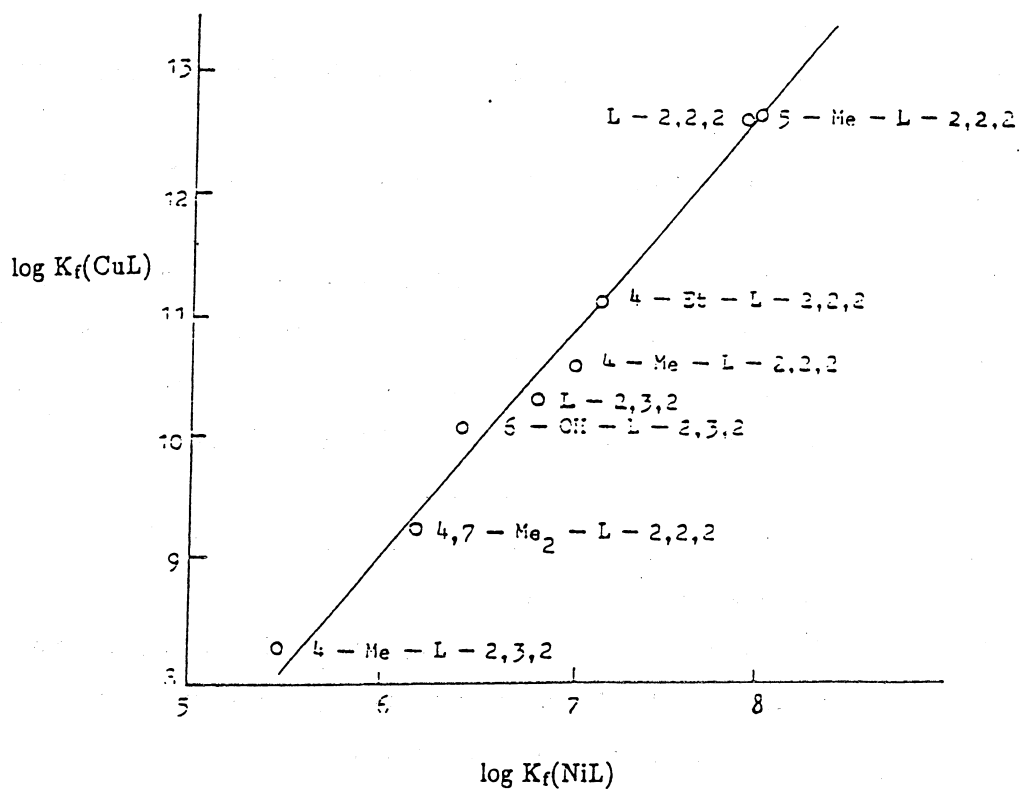


Figure 1.

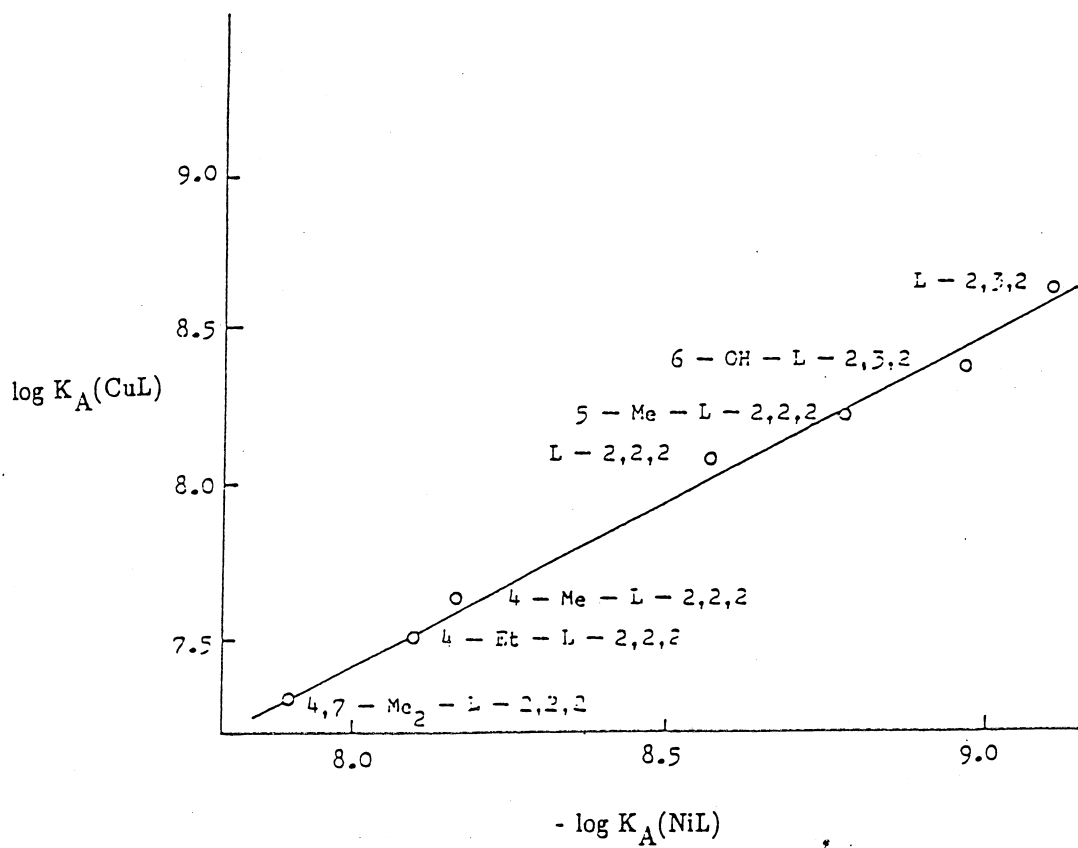


Figure 2.

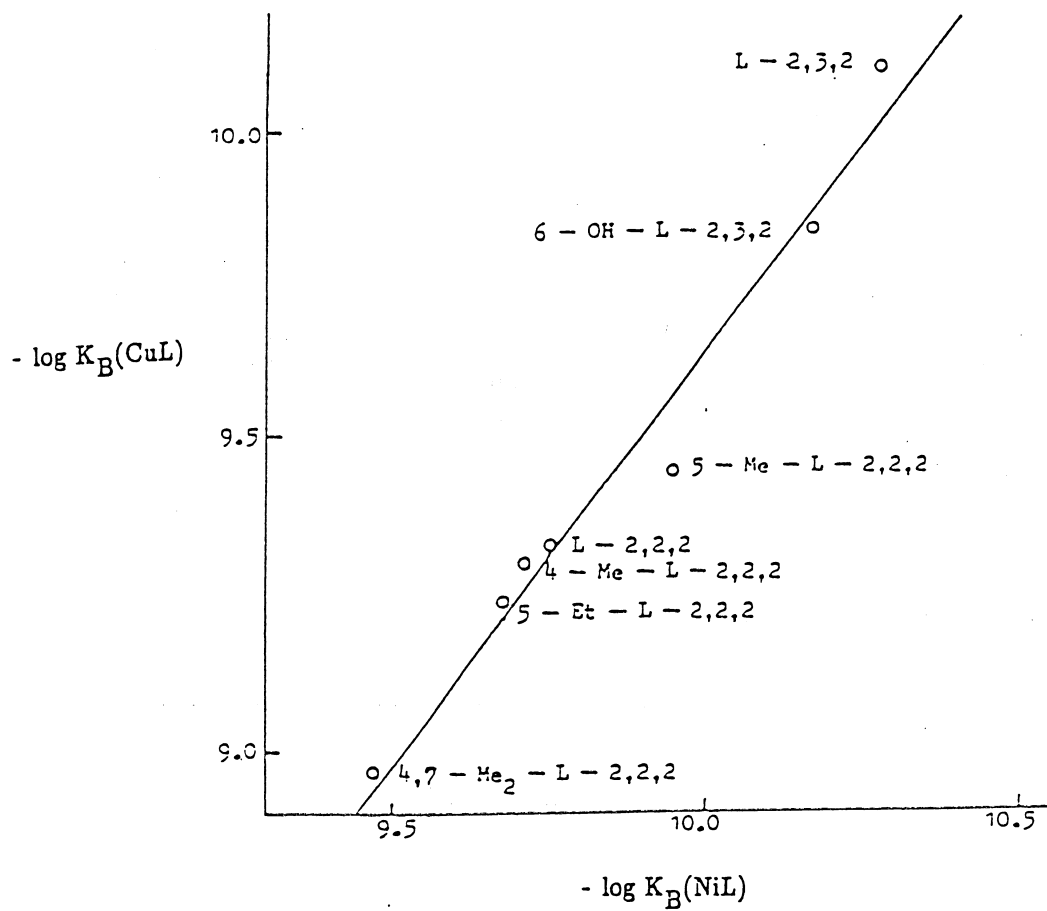
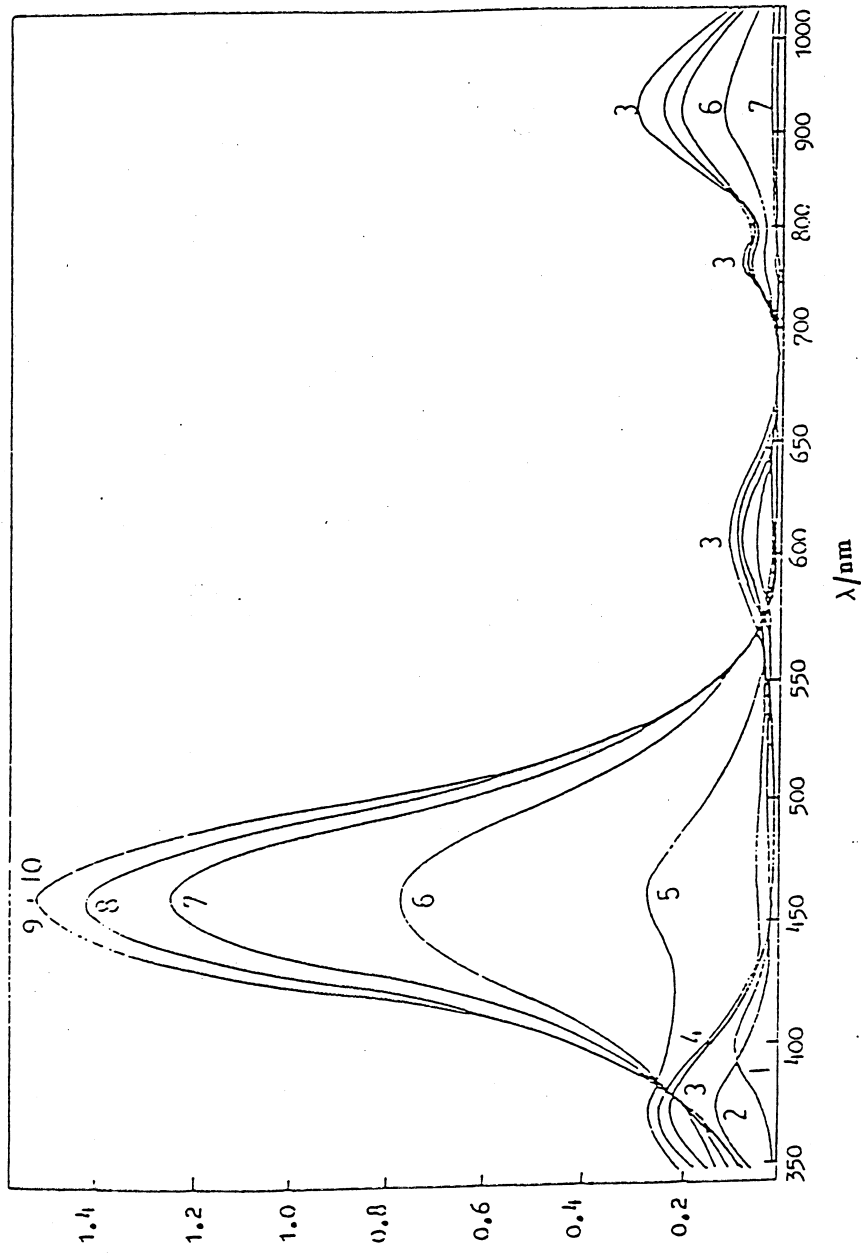


Figure 3.



A

Figure 4.

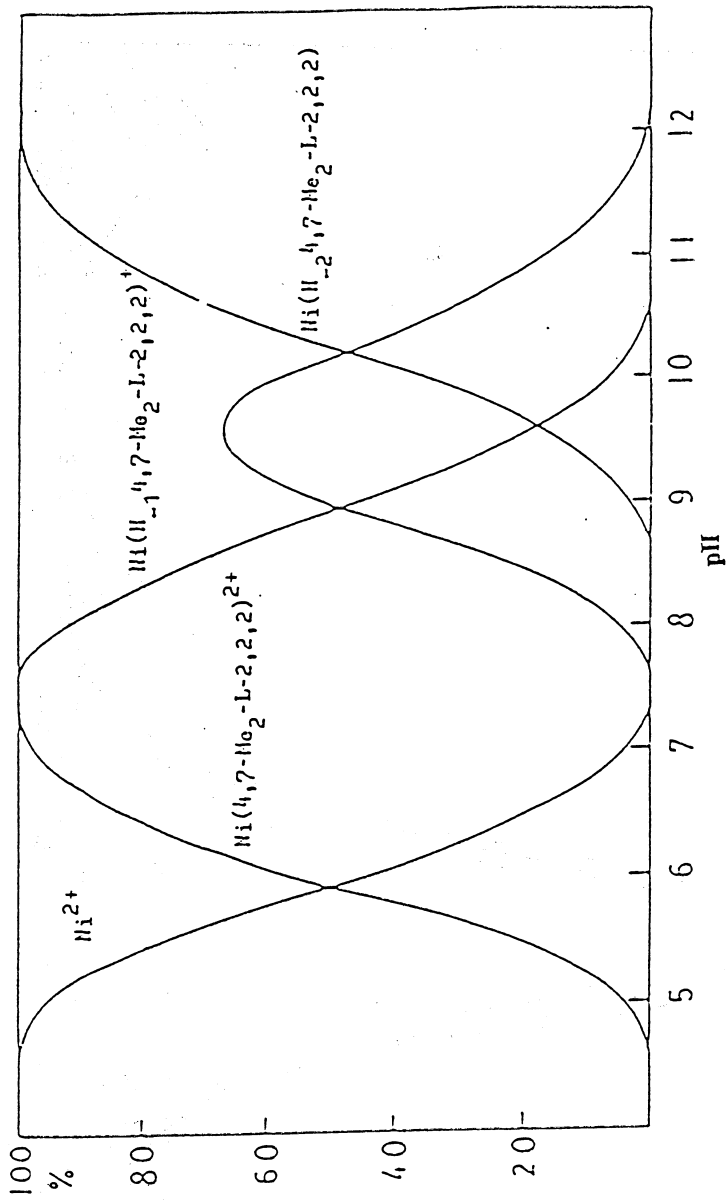


Figure 5.

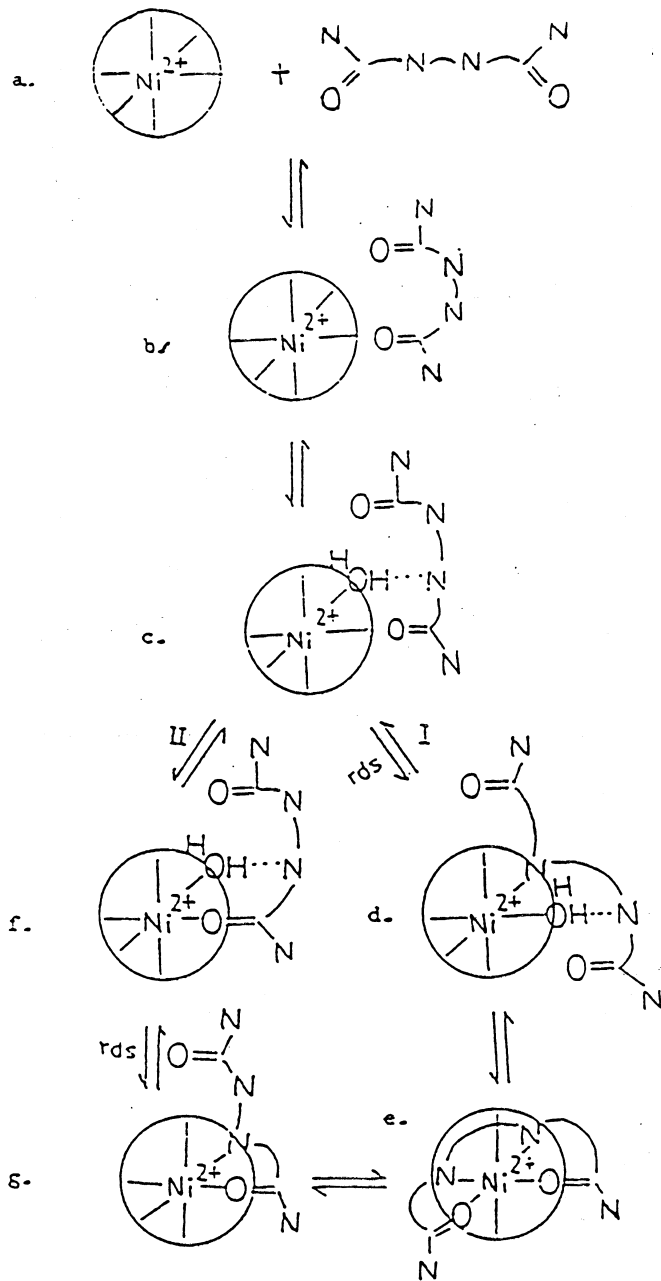


Figure 6.

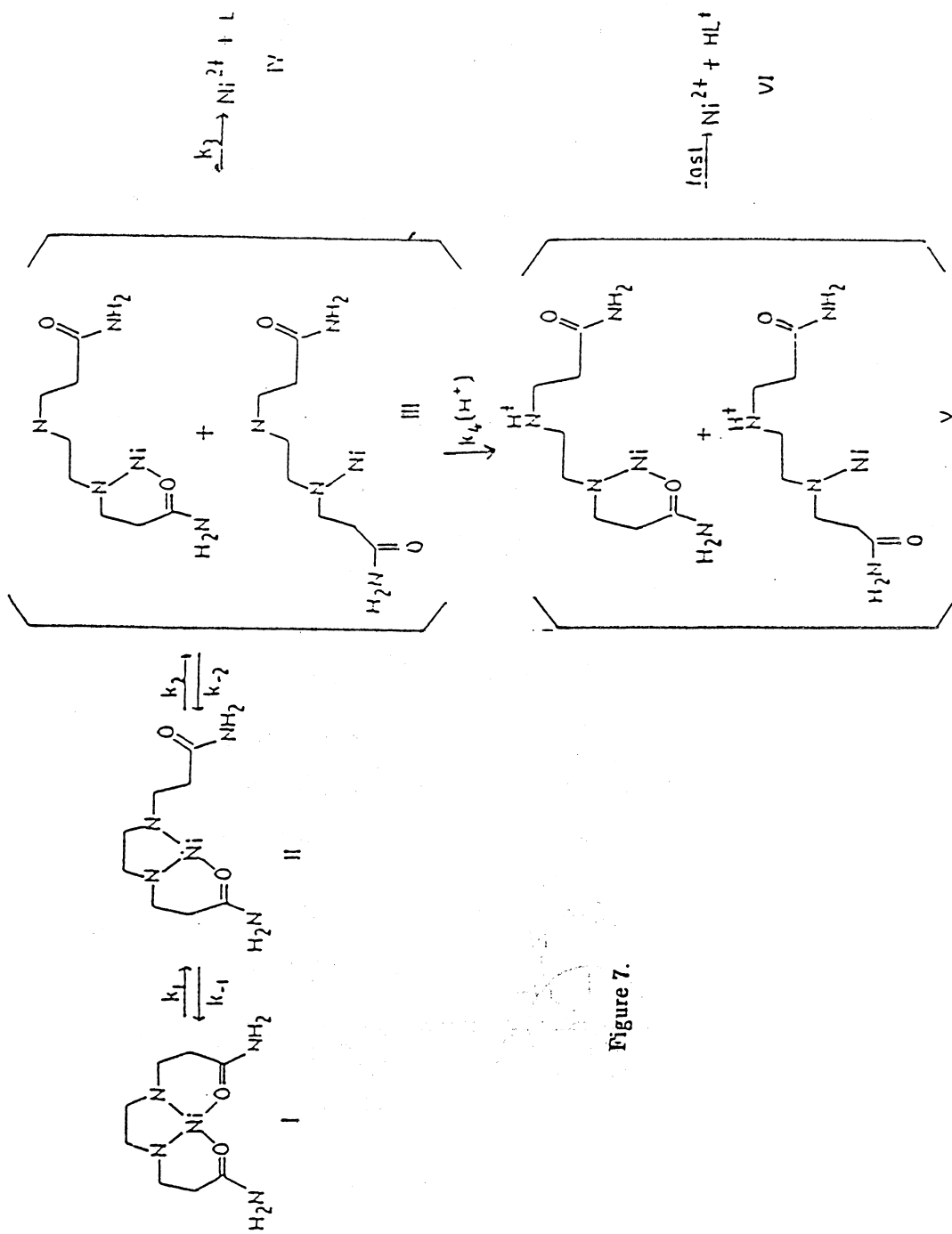


Figure 7.